Design Concept of Supercritical CO_2 Gas Cooled Divertors in FFHR Series Fusion Reactors

Shintaro ISHIYAMA, Akio SAGARA[1)], Hirotaka CHIKARAISHI[1)] and Nagato YANAGI[1)]

School of Fundamental Science and Engineering, Waseda University, 3-4-1 Ohkubo, Shinjyuku-ku, Tokyo 169-8555, Japan

[1)]*National Institute for Fusion Science, 322-6 Oroshi, Toki, Gifu 509-5292, Japan*

(Received 20 April 2022 / Accepted 16 September 2022)

In the FFHR power reactor equipped with a supercritical CO_2 gas turbine power generation system, an divertor cooling system is connected to this power generation system [S. Ishiyama *et al.*, Prog. Nucl. Energy **50**, No.12-6, 325 (2008) [1]]. In this paper, for the purpose of developing a diverter by supercritical CO_2 gas cooling that can cope with a neutron heavy irradiation environment with a heat load of 15 MW/m^2 or more, CFD heat transfer flow analysis was carried out for performance evaluation and its design optimization by a structural analysis models of a supercritical CO_2 gas cooled divertors. As a result, in the supercritical CO_2 gas cooled tungsten mono-block divertors (50×50 mm $\times$ 5 channel $\times$ 5,000 mL) with a flow path length of 5 m or less, the engineering designable range of these advanced diverters having the same cooling performance as the water cooling divertor was clarified, and its practicality is extremely high from the feature that the structural model has an extremely low risk during operation as compared with the water cooled divertor.

Keywords: divertor, super critical CO_2 gas turbine, Force Free Helical Reactor (FFHR), bypass control, axial-flow single-shaft design turbine, CFD, heat transfer flow analysis

DOI: 10.1585/pfr.17.1405103

1. Introduction

The supercritical CO_2 gas turbine power generation system consists of a low / high pressure compressor, a bypass compressor, a gas turbine, a pre- / intermediate heat exchanger and multiple regenerated heat exchangers, and the FFHR power reactor equipped with this power generation system has high-efficiency power generation performance, low construction cost due to its compactness, and high safety during operation [2–6]. Above all, regarding safety during operation, it has the feature of avoiding all of the following risks in the water cooling system.

In a water-cooled fusion device, there are many risks inherent during operation, such as damages to the blanket equipment due to high-pressure generated steam induced when the water coolant leaks from the high-temperature thin tube for cooling in high vacuumed vessel, vapor/hydrogen explosion, replacement with tritium water, oxidative corrosion of high-temperature equipment such as divertor, electric leakage in the electrical system when a large amount of water leaks into the vacuum vessel and prolongation of the vacuum return period due to the residual of leaked water in vacuum chamber after these troubles.

Recently, the authors have proposed a high-efficiency power generation system using the blanket and divertor shown in Fig. 1 as a heat source in order to further utilize these characteristics, a supercritical CO_2 gas-cooled divertor was adopted in the paper [7].

In this paper, the characteristics of the supercritical CO_2 gas-cooled divertor in the FFHR power reactor are evaluated by CDF heat transfer flow analysis, and the engineering design feasibility and optimized design was verified comparing the cooling performance with other cooling media.

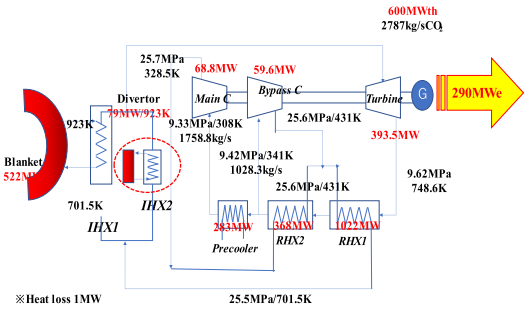

Fig. 1 The 0.6 MWth FFHR power plant connected to Supercritical CO_2 gas turbine system [7].

2. Procedures

The characteristics and performance of the supercritical CO_2 gas-cooled diverter were evaluated by CFD heat transfer flow analysis [5] using the supercritical CO_2 actual gas data [8].

author's e-mail: shintaroishiyama1955@gmail.com

2.1 Heat transfer flow analysis by CFD

2.1.1 Heat transfer flow analysis method

The heat transfer flow analysis of the supercritical CO_2 coolant flowing in the various divertor models shown in (2.2) below was carried out. This analysis was carried out by the heat transfer flow analysis software Fluent ver.18 using NIST's supercritical CO_2 gas actual gas data and physical property data [8] of various components materials of divertors. The transition SST model was applied to the viscosity model. The gravitational acceleration is also taken into consideration [7].

(a) Steady-state heat transfer flow analysis of divertor basic structure models

In order to select the engineering feasibility range of the divertor, CFD steady-state analysis using actual liquid data was performed using the divertor basic structure analysis model in (2.1.2) (a) below with the inlet fluid flow velocity as a parameter. At that time, in order to ensure the supercriticality of the CO_2 coolant during divertor operation, the inlet temperature and outlet pressure in the cooling channel were set to 350 K and 10 MPa, respectively. The heat load input to the armor tile surface of the divertor structure model was set to 15 and 20 MW/m^2.

(b) Steady-state analysis by divertor actual structure analysis models

In the heat transfer flow analysis using the divertor actual structure analysis model in (2.1.2) (b) below, We evaluated the flow characteristics of the material and optimized the divertor structure within the range of the engineering design established in the above (2.1.2) (a) model analysis.

2.1.2 CFD analysis models

2.1.2-1 Basic divertor analysis model

Figure 2 shows the basic divertor model. The basic divertor model (Fig. 2 (a)) is composed of tungsten armor tile (10 mmt × 50 mm × 10,000 mm) (Fig. 2 (a-1)) and ODS substrate with a φ40 cooling channel (50 × 50 × 10,000 mmL, (a)), in which a supercritical CO_2 cooling medium (φ40 × 10000 mmL (a-3)) flows into the cooling channel.

Figure 2 (b) shows a mesh model for heat transfer flow analysis. The cell size is 1275371 and the number of faces and the number of nodes are 490030 and 1460020, respectively.

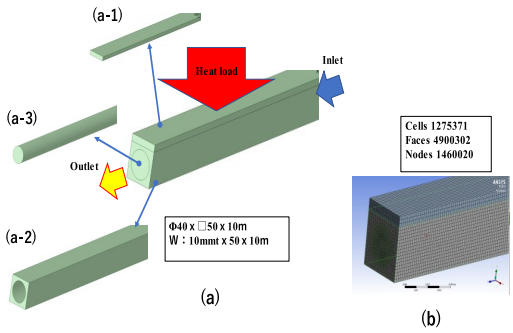

Fig. 2 Basic divertor structure and mesh models for CFD heat transfer analysis.

2.1.2-2 Divertor structure analysis model for CFD heat transfer analysis

(a) Manifold type divertor analysis model

Figure 3 shows the manifold type divertor analysis model in which 15 cooling channels are connected to the manifolds. The basic dimensions and shape specifications are as follows.

Tungsten armor tile: 5 × 1.6 × 0.01 mt

Main Piping: φ300 / 250 (In / Outlet: 3 × 1)

Cooling channel: φ50 mm × 15

ODS Substrate: 5 × 1.6 × 0.1 mt

(b) Panel type divertor analysis model

Figure 4 shows the panel type divertor model. The basic dimensions and shape specifications are the same as in (a) Manifold type analysis model above, and each inlet / outlet manifold is abolished, the flow rate in each inlet pipe can be adjusted evenly, and the outlet side has a single flat plate structure.

(c) Tungsten mono-block divertor analysis model

Figure 5 shows a tungsten mono-block analysis model. The entire divertor structure analysis model was made entirely of tungsten, and five cooling channels (diameter 50 mm × 5000 mm L) were connected to the manifold

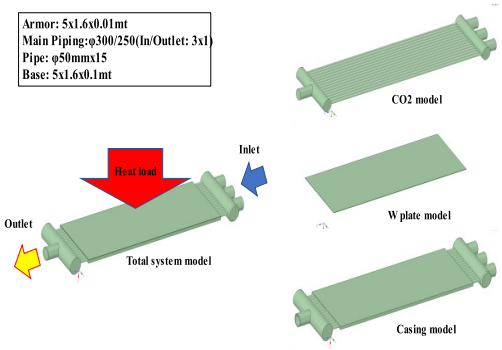

Fig. 3 Manifold type divertor analysis model.

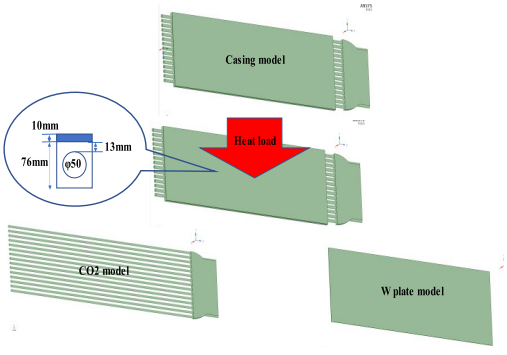

Fig. 4 Panel type divertor analysis model.

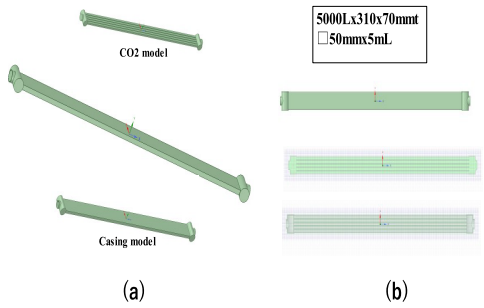

Fig. 5 Tungsten mono-block divertor analysis model.

at the inlet and outlet.

3. Results

In order to verify the feasibility of the engineering design regarding the cooling performance of the analysis case in which supercritical CO_2 gas is selected as the cooling material, comparison of the cooling performance between supercritical CO_2, water and helium cooling were also carried out.

3.1 Heat transfer flow analysis of the basic divertor model

3.1.1 Performance characteristics and engineering design range of supercritical CO_2 gas cooled divertor model

To determine the engineering design scope of the divertor basic model, the parametric heat transfer flow analysis of the supercritical CO_2 gas during 15 and 20 MW/m^2 heat load operation is performed by the inlet flow rate.

Figure 6 shows the temperature distribution under the following flow conditions in the divertor basic model at heat load 15 MW / m^2.

In/Outlet velocity: V_{in} / V_{out}: 70 / 150.9 m / s

In/Outlet pressure P_{in} / P_{out}: 12.86 / 10 MPa

In/Outlet density D_{in} / D_{out}: 353.9 / 173.6 kg / m^3

Mass flow rate: 31.06 kg / s

In/Outlet temperature T_{in} / T_{out}: 350 / 410.8 K

Tungsten armor surface average / maximum temperature: 2401.3 / 2531.7 K

In/Outlet viscosity: 2.78E-5 / 2.31E-5 kg / m-s

According to these results, it can be seen that the surface temperature of the tungsten armor tile surface temperature distribution gradually rises from the cooling channel inlet to the outlet in Fig. 6 (a). The non-uniform temperature distribution on the armor tile can also be confirmed from the temperature distribution in the cross-sectional direction in Fig. 6 (b).

Figures 7 to 11 show the relationship between inlet velocity and temperature, mass flow rate (Figs. 7 and 8 (a) (b)), pressure and outlet velocity (Figs. 9 and 10 (a) (b)) at heat load of 15 and 20 MW/m^2, respectively. The relationship between inlet velocity and the density change is also shown in Figs. 11 (a) (b).

According to these results, the temperature on the divertor decreases due to the increase in the mass flow rate with the increase in the inlet flow velocity, and this tendency tends to increase with the increase in the heat load. At that time, an increase in pressure and flow velocity at the outlet of the divertor and a decrease in density are ob-

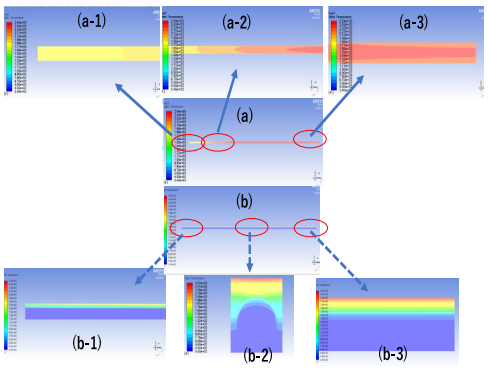

Fig. 6 Temperature distribution of supercritical CO_2 cooled divertor under 15 MW/m^2 heat load.

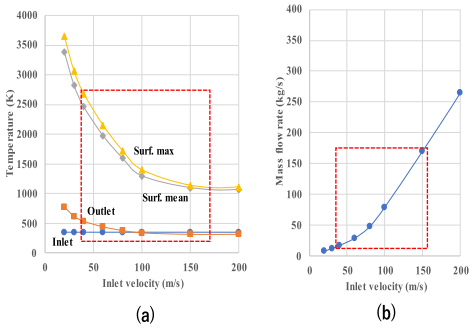

Fig. 7 The relationship between inlet velocity and temperature (a), and mass flow rate (b) of supercritical CO_2 cooled divertor under 15 MW/m^2 heat load.

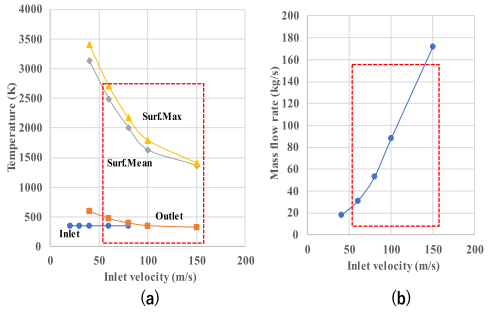

Fig. 8 The relationship between inlet velocity and temperature (a), and mass flow rate (b) of supercritical CO_2 cooled divertor under 20 MW/m^2 heat load.

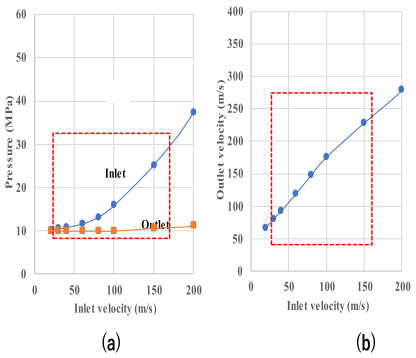

Fig. 9 The relationship between inlet velocity and pressure (a), and outlet velocity (b) of supercritical CO_2 cooled divertor under 15 MW/m^2 heat load.

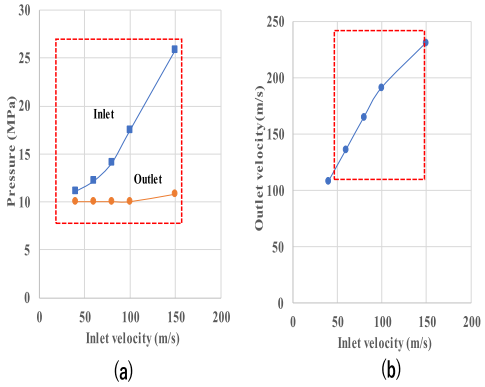

Fig. 10 The relationship between inlet velocity and pressure (a), and outlet velocity (b) of supercritical CO_2 cooled divertor under 20 MW/m^2 heat load.

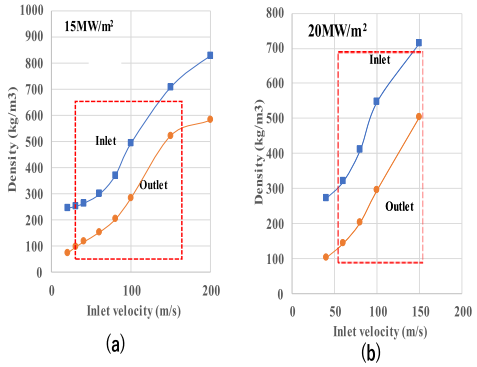

Fig. 11 The relationship between inlet velocity and density of supercritical CO_2 cooled divertor under 15 (a) and 20 MW/m^2 (b) heat load.

served.

Here, the design condition range of the divertor basic model is set by the following engineering design conditions.

(1) Maintaining a supercritical state under divertor operation conditions

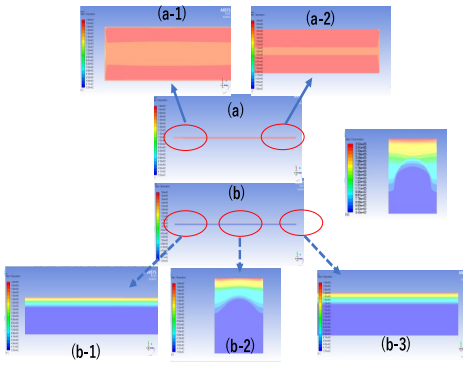

Fig. 12 Temperature distribution of water cooled divertor under 15 MW/m^2 heat load.

The critical temperature and pressure must be equal to or higher than the following values.

- Critical temperature > 304.1 K
- Critical pressure > 7.38 MPa

(2) Must be within the usable temperature range of the divertor component equipment

The conditions for using the constituent materials, tungsten and ODS materials are shown below.

- Limit temperature for tungsten: below melting point (< 3683 K)

*Tungsten recrystallization temperature: 1500 - 1800 K

- Limit temperature for ODS (0.13C-9Cr-2W-0.2Ti/Y_2O_3) < 973 K [9–12]

Here, the temperature range in which the divertor can be operated that simultaneously satisfies both the above conditions (1) and (2) is shown by the broken line frame in Figs. 7 to 11. It can be seen that this setting operation range is slightly shifted to the higher velocity side of the inlet flow velocity at 20 MW / m^2 with respect to the heat load of 15 MW / m^2.

3.1.2 Heat removal characteristics of water cooled divertor

Figure 12 shows the cooling performance of the water cooled divertor with a heat load of 15 MW / m^2 under the same flow conditions (same as the inlet flow velocity / outlet pressure conditions) as the supercritical CO_2 gas cooling divertor described in (3.1.1) above.

According to this, it can be seen that the surface temperature of the armor tile rises unevenly from the vicinity of the inlet to the outlet as in the supercritical CO_2 gas cooling (Figs. 12 (a-1) (a-2)). However, the temperature distribution in the cross-sectional direction of the cooling channel (Figs. 12 (b-1) to (b-3)) does not show the non-uniformity of the temperature distribution as seen in the supercritical CO_2 gas cooled divertor.

3.1.3 Helium-cooled heat removal performance characteristics

The results of the cooling performance evaluation of the helium cooled diverter under the same conditions as the above water cooled divertor (3.1.1) are shown below.

In/Outlet velocity: V_{in} / V_{out}: 70 / 73.6 m / s

In/Outlet pressure P_{in} / P_{out}: 1.00013 / 10 MPa

In/Outlet density D_{in} / D_{out}: 0.1625 / 0.1625 kg / m^3

Mass flow rate: 0.0143 kg / s

In/Outlet temperature T_{in}/T_{out}: 350/5000 K

Armor surface average/maximum temperature:

5143.7 / 5143.7 K

Viscosity: 1.99E-5 kg / m-s

As a result of this analysis, it can be seen that the cooling mechanism of the divertor structure model using helium is not functioning because the helium mass flow rate into the cooling channel is not sufficiently secured under the same operating conditions as the supercritical CO_2 gas cooled divertor.

From this result, it can be concluded that in order to make the cooling mechanism functional in the helium cooled divertor, it is necessary to increase the inlet pressure much higher than that in the supercritical CO_2 gas cooled divertor.

4. Discussion

4.1 Heat removal performance characteristics of supercritical CO_2 gas cooled divertor

From the result of (3.1) above, in the supercritical CO_2 gas cooled divertor, the heat load between the inlet and outlet of the cooling channel affects the fluctuation of the armor tile surface temperature, the supercritical CO_2 gas temperature and its flow velocity with the remarkable fluctuation of density and flow velocity.

Here, Fig. 13 shows the changes in the temperature distribution that occur in the longitudinal direction of the cooling channel (10 mL) due to the supercritical CO_2 gas cooled divertor and the changes in various thermophysical properties.

According to this, in the case of the supercritical CO_2 gas cooled divertor, it can be seen that the fluid temperature rises as a result of the decrease in heat removal performance because the fluid density decreases with the decrease in pressure along the channel flow path. On the other hand, it can be seen that the pressure is reduced as a result of the decrease in viscosity.

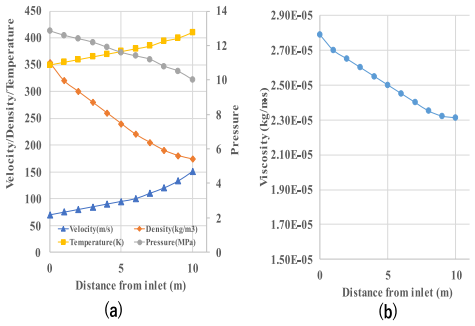

Fig. 13 Change in velocity, density and temperature (a) and viscosity (b) as a function of distance from inlet of supercritical CO_2 cooled divertor under 15 MW/m^2 heat load.

4.2 Comparison of cooling performance with various coolants

Figures 14 (a) to (e) show the comparison results of the cooling performance analysis results for various cooling media under 15 MW/m^2 heat load.

In the flow velocity and density change (Figs. 14 (a)

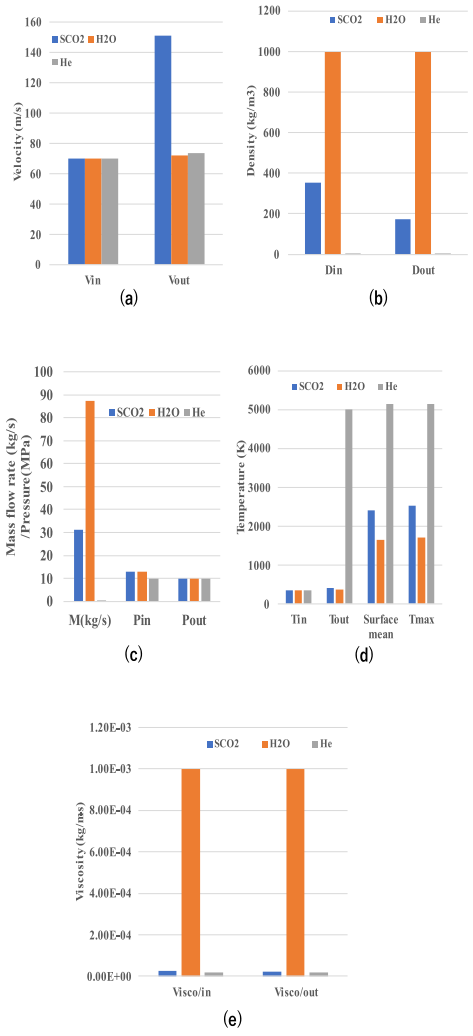

Fig. 14 Comparison between supercritical CO_2 cooling, water and helium cooling method of velocity (a), density (b), mass flow rate/pressure (c), temperature (d) and viscosity (e) at in/outlet of basic divertor model under 15 MW/m^2 heat load.

(b)) in each cooling method under the same operating conditions, the supercritical CO_2 gas cooling method has an outlet velocity that is more than twice the inlet speed, whereas the velocity change in the water and helium cooling methods is small.

On the other hand, regarding the density change at the inlet and outlet, the density change hardly occurs at this operating temperature in the water cooling method, whereas in the case of supercritical CO_2 gas, it decreases to about half at the outlet with respect to the inlet.

In the cooling fluid mass flow rate and pressure change (Fig. 14 (c)), the mass flow rate in the water cooling method is more than three times higher than that in the supercritical CO_2 cooling method. This suggests that the cooling performance is not significantly impaired even if the inlet pressure is further reduced in the water cooling method.

Figure 14 (d) shows the divertor inlet / outlet temperature by various cooling methods and the average and maximum temperature on the armor tile surface.

According to this, it can be seen that the cooling method other than helium has realized the low temperature of the armor tile and the cooling material that satisfy the engineering design establishment condition of (3.1.1).

Among them, the cooling performance for armor tiles, especially in the case of water cooling, is higher than that of the supercritical CO_2 gas cooling method, which is due to the increased flow rate of the water coolant in Fig. 14 (c).

Therefore, if the heat removal performance at the same mass flow rate is compared between the supercritical CO_2 gas cooling and the water cooling method, it is considered that both have almost the same cooling performance.

On the other hand, the cooling performance during the same operation in the helium cooling method could not be obtained at all due to insufficient mass flow rate, so it was decided to exclude it from the following options.

Regarding the change in fluid viscosity in Fig. 14 (e), although no significant change was observed at the inlet and outlet in each cooling method, the water cooling method had a relatively high numerical value compared to the supercritical CO_2 gas cooling method.

4.3 Heat transfer flow characteristics of the actual divertor model

Here, the heat transfer flow analysis of various supercritical CO_2 gas cooled actual structure divertor models under the operating conditions within the engineering design range of (3.1.1) was performed and the performance characteristics of each were evaluated.

4.3.1 Supercritical CO_2 gas cooled manifold type diverter

Figure 15 shows the results of heat transfer flow analysis under a 15 MW/m^2 heat load of a manifold type diverter

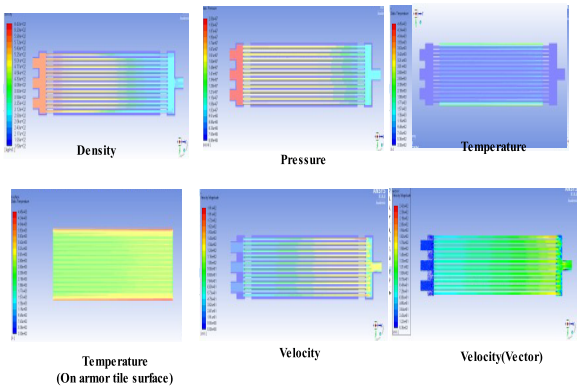

Fig. 15 Flow status of supercritical CO_2 gas in manifold type divertor under 15 MW/m^2 heat load.

with 15 cooling channels connected.

According to this, it can be seen that as a result of the non-uniformity of the coolant distributed from the inlet manifold to each cooling channel, high temperature portions are generated at both ends of the equipment including the armor tile surface.

The analysis results of this model are shown below.

In/Outlet velocity: V_{in} / V_{out}: 14.09 / 108.3 m / s

In/Outlet pressure P_{in} / P_{out}: 19.93 / 10 MPa

In/Outlet y density D_{in} / D_{out}: 616 / 247.8 kg / m^3

Mass flow rate: 1279.3 kg / s

In/Outlet temperature T_{in} / T_{out}: 349.8 / 346.5 K

Armor surface average/maximum temperature: 2450 / 2643 K

It can be seen that the cooling capacity of this analysis model is almost the same as that of the divertor basic structure model in (3.1.1), but because of the manifold and multiple pipe connection in this model, and also it can be seen that the inlet pressure is about 1.5 times higher than that of the above divertor basic structure model in order to compensate for the pressure loss that occurs in cooling channels.

4.3.2 Supercritical CO_2 gas cooled plate type divertor

As an improvement method to eliminate the high temperature part at both ends caused by the above manifold type diverter and to reduce the pressure loss resistance generated in the manifold while lowering the surface temperature of the armor tile, both the inlet and outlet manifold are eliminated, and 15 pipes are replaced. These pipe were individually controlled to adjust the mass flow rate so that the coolant flows evenly to each cooling channel at the inlet and a plate-type single outlet pipe was installed instead of the outlet manifold.

The results of heat transfer flow analysis of the plate-type divertor are shown in Figs. 16 and 17, respectively.

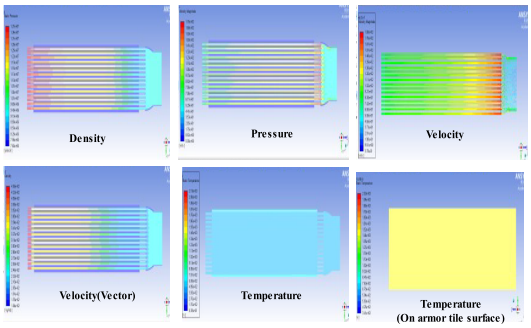

Fig. 16 Flow status of supercritical CO_2 gas in flat plate type divertor under 15 MW/m^2 heat load.

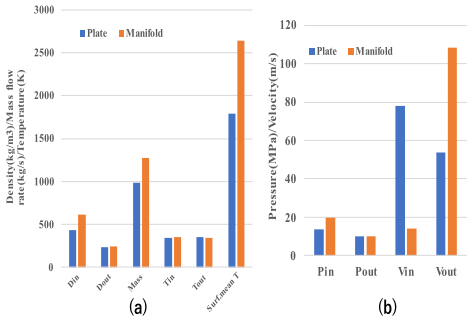

Fig. 17 Comparison in density/mass flow rate/temperature (a) and pressure/velocity at in/outlet divertor between plate and manifold type divertor under 15 MW/m^2 heat load.

From these results, it can be seen that the non-uniform temperature distribution on the surface of the armor tile is eliminated by the above-mentioned improvement (Fig. 16). In addition, from the results shown in Fig. 17, it can be seen that in the plate-type diverter, the inlet density, flow rate, and armor average temperature were significantly reduced and improved, and the inlet pressure was reduced by increasing the inlet velocity.

4.3.3 Divertor optimization design

Since the recrystallization temperature of tungsten armor tiles is 1500 to 1800 K [11–13], it is desirable that the armor tar surface temperature during operation be maintained below this temperature range.

Therefore, here, we investigated the optimization of the length in the direction of the divertor flow path. Figure 18 shows the maximum temperature of the armor tile surface and the change in supercritical CO_2 gas temperature in the longitudinal direction of the divertor model under a heat load of 15 MW / m^2.

According to this, it can be seen that the armor tile surface temperature can be suppressed to the above-mentioned recrystallization temperature or less by shortening the length of the divertor flow path to 5 m or less in order to prevent the recrystallization of tungsten during the divertor operation.

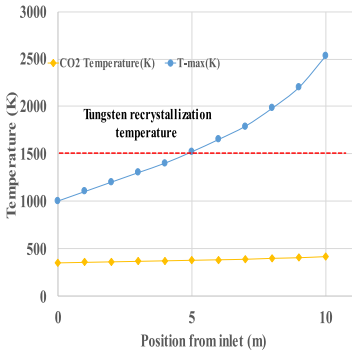

Fig. 18 Maximum temperature of the armor tile surface and the change in supercritical CO_2 gas temperature in the longitudinal direction of the divertor model under a heat load of 15 MW/m^2.

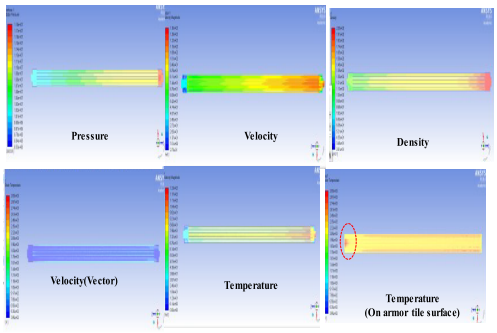

Fig. 19 Flow status of tungsten mono-block divertor at supercritical CO_2 gas inlet flow rate of 40 m/s under a load of 15 MW/m^2.

4.3.4 Cooling performance evaluation of high radiation compatible divertor structure model

It has been pointed out that in the actual divertor, material deterioration occurs when it is exposed to heavy neutron irradiation of 14 MeV with a high heat load. In particular, it has been pointed out that the ODS material causes significant deterioration in characteristics that interferes with long-term operation when exposed to irradiation of about 20 dpa within the expected operation period [3, 9–13].

Therefore, here, the heat removal performance evaluation by supercritical CO_2 gas cooling is performed using the tungsten mono-block structure diverter (5 mL length × 310 mm W × 70 mmt, 50 mm×50 mm × 5 channels) shown in Fig. 5, which has high resistance to radiation damage for long-term operation.

Figure 19 shows the results of heat transfer flow analysis at a supercritical CO_2 gas inlet flow rate of 40 m/s under a load of 15 MW/m^2. Figure 20 shows the comparison results of heat removal performance when the inlet flow velocity is increased from 40 m/s to 80 m/s under 15 MW/m^2 and 20 MW/m^2 high heat load at 80 m/s, respectively.

According to this, a hot spot shown in the broken

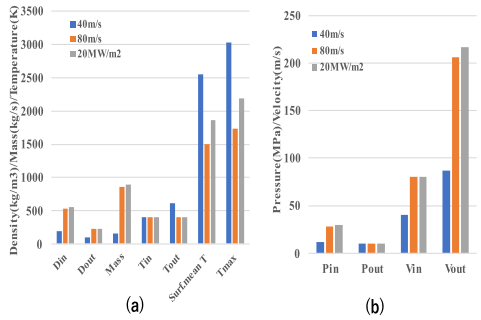

Fig. 20 Comparison in density/mass flow rate/temperature (a) and pressure/velocity (b) of in/outlet of supercritical CO_2 cooled tungsten mono-block divertor at inlet velocity 40 and 80 m/s under 15 and 20 MW/m^2 heat load.

line frame in Fig. 19 is generated near the surface inlet of the tungsten mono-block divertor under a heat load of 15 W/m^2 at a flow velocity of 40 m/s, and the local maximum surface temperature there exceeds 3000 K, which can be seen from the results in Fig. 20 (a).

On the other hand, it is confirmed from the result of Fig. 20 (a) that this local maximum surface temperature and surface average temperature are suppressed to 2000 K or less when the flow velocity is increased to 80 m/s under a heat load of 15 MW/m^2. On the other hand, in the case of the heat load of 20 MW/m^2 × 80 m/s in Fig. 20 (a), the surface average temperature is suppressed to 2000 K or less, although there is a possibility of local damage due to local aria exceeding 2000 K.

5. Conclusions

Aiming to develop a nuclear fusion reactor diverter that can handle high heat load of 15 to 20 MW / m^2 and heavy irradiation, performance evaluation and optimization design of advanced diverter structure model by supercritical CO_2 gas cooling method is carried out by CFD heat transfer flow analysis based on supercritical CO_2 actual gas data and the flowing results are derived,

(1) The engineering designable range and operating conditions was set for The supercritical CO_2 gas cooled diverter.
(2) As a result of performance comparison evaluation of water cooling and helium gas cooling method in addition to supercritical CO_2 gas cooling method, the water cooling method operates at a relatively low pressure compared to the supercritical CO_2 gas cooling method. Although it is considered possible, the viscosity is much higher than that of the supercritical CO_2 gas cooling method, so higher compression and pressurization power than that of the supercritical CO_2 gas cooling method is required.
(3) On the other hand, the helium cooling method has no choice but to operate at a considerably higher pressure than the supercritical CO_2 gas cooling method and the water cooling method.
(4) As an advanced diverter that can handle high heat load of 15 to 20 MW/m^2 and heavy irradiation and has higher safety, a supercritical CO_2 gas cooling tungsten mono-block diverter (50×50 mm×5 channel ×5,000 mL) with a flow path length of 5 m or less is promising.

Acknowledgments

Part of this research was conducted under the NIFS Collaborative Research Program NIFS21KERA019.

[1] S. Ishiyama, Y. Muto, Y. Kato, S. Nishio, T. Hayashi and Y. Nomoto, Prog. Nucl. Energy **50**, No.12-6, 325 (2008).
[2] A. Sagara, H. Tamura, T. Tanaka, N. Yanagi, J. Miyazawa, T. Goto, R. Sakamoto, J. Yagi, T. Watanabe, S. Takayama and the FFHR design group, Helical reactor design FFHR-d1 and c1 for steady-state DEMO, Fusion Eng. Des. **89**, 2114 (2014).
[3] A. Sagara, J. Miyazawa, H. Tamura, T. Tanaka, T. Goto, N. Yanagi, R. Sakamoto, S. Masuzaki, H. Ohtani and The FFHR Design Group, Two conceptual designs of helical fusion reactor FFHR-d1A based on ITER technologies and challenging ideas, Nucl. Fusion **57**, 086046 (2017).
[4] A. Sagara, T. Tanaka, J. Yagi, M. Takahashi, K. Miura, T. Yokomine, S. Fukada and S. Ishiyama, Fusion Sci. Technol. **68**, 303 (2015).
[5] S. Ishiyama, H. Chikaraishi and A. Sagara, Operating scenario of 3GWth class FFHR power plant with bypass controlled supercritical CO_2 gas turbine power generation system, Fusion Eng. Des. **164**, 112194 (2021).
[6] S. Ishiyama, T. Tanaka, A. Sagara and H. Chikaraishi, Fusion Sci. Technol., DOI: https://doi.org/10.1080/15361055.2019.1658046 (2019).
[7] S. Ishiyama, H. Chikaraishi and A. Sagara, Up-grade Bypass controlled supercritical CO_2 gas turbine for 0.6MW$_{th}$ FFHR series fusion reactors, Plasma Fusion Res. **17**, 2405054 (2022).
[8] https://www.nist.gov.
[9] F.A. Garner and M.L. Hamilton, JNM **191-194**, 386 (1992).
[10] D.J. Edwards *et al.*, JNM **191-194**, 416 (1992).
[11] M. Tokitani, S. Masuzaki, Y. Hiraoka *et al.*, Potential of Copper Alloys using a Divertor Heat Sink in the Helical Reactor FFHR-d1 and their Brazing Properties with Tungsten Armor by using the Typical Candidate Filler Materials, Plasma Fusion Res. **10**, 3405035 (2015).
[12] J. Reiser, M. Rieth, B. Dafferner and A. Hoffmann, Divertor from the technology perspective, 1st IAEA DEMO program workshop, 15-18 October 2012.
[13] A. Sagara, T. Goto, J. Miyazawa, N. Yanagi *et al.*, Full report on the NIFS fusion engineering research project for the mid-tem of FY2010-2015, National Institute for Fusion Science.